Complex Formation of Bovine Serum Albumin with a Poly(ethylene glycol) Lipid Conjugate

Valeria Castelletto* and Marta Krysmann

The University of Reading, Department of Chemistry, P.O. Box 224, Whiteknights, Reading RG6 6AD, United Kingdom,

Antonios Kelarakis

National and Kapodistrian University of Athens, Department of Chemistry, Physical Chemistry Laboratory, Panepistimiopolis, 157 71 Athens, Greece

Paula Jauregi

The University of Reading, School of Food Biosciences, P.O. Box 226, Whiteknights, Reading RG6 6AP, United Kingdom

Received January 30, 2007; Revised Manuscript Received May 8, 2007

In this work, we report the formation of complexes by self-assembly of bovine serum albumin (BSA) with a poly(ethylene glycol) lipid conjugate (PEG_{2000}-PE) in phosphate saline buffer solution (pH 7.4). Three different sets of samples have been studied. The BSA concentration remained fixed (1, 0.01, or 0.001 wt % BSA) within each set of samples, while the PEG_{2000}-PE concentration was varied. Dynamic light scattering (DLS), rheology, and small-angle X-ray scattering (SAXS) were used to study samples with 1 wt % BSA. DLS showed that BSA/PEG_{2000}-PE aggregates have a size intermediate between a BSA monomer and a PEG_{2000}-PE micelle. Rheology suggested that BSA/PEG_{2000}-PE complexes might be surrounded by a relatively compact PEG-lipid shell, while SAXS results showed that depletion forces do not take an important role in the stabilization of the complexes. Samples containing 0.01 wt % BSA were studied by circular dichroism (CD) and ultraviolet fluorescence spectroscopy (UV). UV results showed that at low concentrations of PEG-lipid, PEG_{2000}-PE binds to tryptophan (Trp) groups in BSA, while at high concentrations of PEG-lipid the Trp groups are exposed to water. CD results showed that changes in Trp environment take place with a minimal variation of the BSA secondary structure elements. Finally, samples containing 0.001 wt % BSA were studied by zeta-potential experiments. Results showed that steric interactions might play an important role in the stabilization of the BSA/PEG_{2000}-PE complexes.

Introduction

Complexation of proteins with water-soluble synthetic polymers in aqueous media has been extensively studied during the past decades because of their great importance in a variety of chemical[1−3] and biological processes.[4,5]

Serum albumin is the most abundant protein in blood plasma. Early light scattering[6−8] and X-ray scattering experiments[9] proposed an oblate ellipsoid with dimensions of 140 × 40 Å. Later studies, using ^{1}H NMR[10] and X-ray crystallography,[11] indicated that the albumin presents a heart-shaped structure rather than an ellipsoidal shape.

Within the family of serum albumins, bovine serum albumin (BSA) has been taken as a model protein to study the complexation of proteins with water-soluble polymers because of the extensive information available on BSA properties in solution[12−14] and because it can be produced at industrial scale. Polyethylene glycol (PEG) is one of the water-soluble polymers that binds BSA.[15] PEG has a particular relevance because of the wide range of its applications in the pharmaceutical industry and biotechnology, such as the formulation of laxatives, skin creams, or PEGylated therapeutic proteins.[16] However, only one work[17] has been reported in the literature about the spontaneous complexation of BSA with PEG in diluted aqueous solutions.

In view of the limited literature on the subject against the wide range of its potential applications, it is worthy to pursue the search for formulations of hybrid BSA/PEG complexes which can represent an alternative to pure BSA/PEG complexes. Therefore, in this paper, we study the complexation between BSA and a PEG-lipid conjugate, namely, 1,2-distearoyl-*sn*-glycero-3-phosphoethanolamine-*N*-[methoxy(polyethylene glycol)-2000] (PEG_{2000}-PE), in a buffer solution at pH 7.4.

PEG_{2000}-PE conjugates are made by a hydrophilic polyethylene glycol block (PEG_{2000}) and a hydrophobic phospholipid block (PE). The behavior of the PEG_{2000}-PE system in aqueous solution has already been studied elsewhere.[18−20] It is known that PEG_{2000}-PE conjugates self-assemble in the form of micelles in aqueous solutions for concentrations higher than the critical micellar concentration (cmc). In particular, cmc for this molecule is relatively low, that is, 1.37×10^{-3} wt % PEG_{2000}-PE at 25 °C.[18]

The phospholipid block in the PEG_{2000}-PE conjugate carries a negative charge in an aqueous solution at neutral pH, while BSA presents a net negative charge at pH = 7.[21] It is expected that in the BSA/PEG_{2000}-PE/water system at pH 7.4, the PE block forms a compact shell around the BSA (which has the ability to bind anionic surfactants[22] and fatty acids[23] at neutral pH), while the PEG block remains exposed to the water, leading to the formation of a hybrid BSA/PEG aggregate.

In this work, we present a comprehensive characterization of the complexation of PEG_{2000}-PE with BSA. Dynamic light

* To whom correspondence should be addressed. Tel: 44 113 343 7595; fax: 44 113 343 6551; e-mail: V.Castelletto@reading.ac.uk.

10.1021/bm070116o CCC: $37.00
Published on Web 06/22/2007

Scheme 1. Chemical Structure of PEG_{2000}-PE

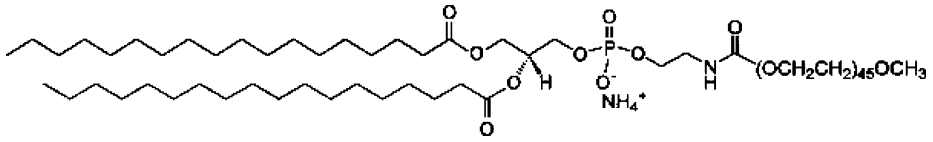

scattering (DLS) and small-angle X-ray scattering (SAXS) were used to have access to the size of the protein/polymer−lipid conjugate complexes. Rheology was used to differentiate between the different morphologies of the objects in the system. The presence of micelles, globular proteins, or protein/polymer complexes has been identified via the determination of the viscosity of the solution. Ultraviolet fluorescence spectroscopy (UV) was used to get an insight into the nature of the forces involved in the interactions between the protein and the polymer. Changes in the secondary structure of the BSA upon complexation with the PEG_{2000}-PE were monitored using circular dichroism spectroscopy (CD). Measurements of electrophoretic mobility (zeta-potential) were used to study the adsorption of PEG_{2000}-PE on the protein surface.

Experimental Section

Materials. BSA and phosphate buffer saline (PBS, pH 7.4, ionic strength $I = 0.169$ M) were obtained from Sigma (United States), while PEG_{2000}-PE was purchased from Avanti Polar Lipids (United States). All the chemicals were used as received without further purification. Scheme 1 shows the chemical structure of PEG_{2000}-PE.

Both BSA (M_{BSA}= 66 000 g mol^{-1}) and PEG_{2000}-PE ($C_{133}H_{267}N_2O_{55}P$, $M_{PEG2000-PE} = 2806$ g mol^{-1}) are negatively charged in aqueous solution at pH 7.4.

Samples were made by first extensively mixing controlled amounts of PEG_{2000}-PE in PBS at pH 7.4. Then, BSA was added to the aqueous PEG_{2000}-PE solution for particular concentration fractions $\Delta = c_{PEG2000-PE}/c_{BSA}$, where each concentration was measured in g/g. BSA/PEG_{2000}-PE solutions were mixed for a period of time and were left to rest for 1 h before undertaking the experiments. During the experiments, the parameter Δ was varied by keeping c_{BSA} constant and increasing $c_{PEG2000-PE}$.

As mentioned in the Introduction, a set of different experimental techniques have been used to study the formation of protein/PEG-lipid conjugate aggregates. Different techniques are sensitive to different concentrations of BSA and therefore give access to the structure of the system for values of Δ with different c_{BSA}. Samples studied by DLS, SAXS, and rheology are in the Δ_1 range, with fixed 1 wt % BSA and variable PEG_{2000}-PE concentration. Samples with fixed 0.01 wt % BSA and variable PEG_{2000}-PE concentration are in the Δ_2 range and have been studied by UV and CD. Finally, samples studied by zeta-potential correspond to the Δ_3 range, with a fixed 0.001 wt % BSA concentration and variable PEG_{2000}-PE concentration. The value of the parameter Δ used in each experiment is detailed in the next section. All the experiments were carried out at 20 °C.

DLS. Experiments were performed using an ALV CGS-3 system with 5003 multidigital correlator. The light source was a 20 mW He−Ne laser, linearly polarized, with $\lambda = 633$ nm. Scattering angles in the range $40 \le \theta \le 150°$ were used for all the experiments. Samples were filtered through 0.20 μm Anotop filters from Whatman into standard 0.5 cm diameter cylindrical glass cells.

DLS experiments measured the intensity correlation function of the radiated light $g^{(2)}(q,t)$:[24]

$$g^{(2)}(q,t) = 1 + A[g^{(1)}(q,t)]^2 \qquad (1)$$

where A accounts for a correction factor depending on the alignment of the instrument, $q = [4\pi n \sin(\theta/2)]/\lambda$ is the scattering vector (λ = vacuum wavelength of the radiation and n = refractive index of the medium), t is the delay time, and $g^{(1)}(q,t)$ is the electric field correlation function.

The program CONTIN can be used to determine the relaxation rate distribution of the system[25] through the modeling of the field correlation function according to:

$$g^{(1)}(t) = \int_0^\infty G(\Gamma) \exp(-\Gamma t) d\Gamma \qquad (2)$$

where $G(\Gamma)$ is the relaxation rate distribution. CONTIN allows for the inverse Laplace transform in eq 2 and provides a tool for calculating the diffusion coefficient of the system. The relaxation rate distributions for different scattering vectors can be used to construct a plot of $\bar{\Gamma}$ versus q^2 (where, for a unimodal distribution, $\bar{\Gamma}$ is taken as the decay rate corresponding to the maximum in $G(\Gamma)$). The mutual diffusion coefficient is calculated as the slope $D = \bar{\Gamma}/q^2$, and it enables the apparent hydrodynamic radius R_H to be calculated according to the Stokes−Einstein equation:

$$R_H = \frac{k_B T}{6\pi\eta D} \qquad (3)$$

where $k_B = 1.38 \times 10^{-23}$ J K^{-1} is the Boltzmann constant and η is the viscosity of water, taken to be $\eta = 1.003 \times 10^{-3}$ Pa s at 20 °C. Equation 3 can also be used to plot the distribution function G in eq 2 as a function of the particle radius (where, for a unimodal distribution, $\bar{R}_H$ is taken as the radius corresponding to the maximum in $G(R_H)$).

SAXS. Experiments were carried out on beamline 2.1 at the Synchrotron Radiation Source (SRS, Daresbury, United Kingdom). The samples were mounted in sealed 1 mm thick liquid cell, with an inner spacer ring to hold liquids, sealed between mica windows.

A wavelength λ of 1.5 Å was used at the SRS together with a multiwire gas-filled area detector. The SAXS data were corrected to allow for sample transmission, background scattering, and detector response. To analyze the data from the two-dimensional detector, the SAXS data was reduced by integration in a radial circular mask (isotropically averaged intensity $I(q)$, where $q = [4\pi \sin(\theta/2)]/\lambda$ is the scattering vector).

The SAXS intensity $I_s(q)$ of a solution corresponding to a system of weakly interacting spherical objects can be approximated at very low scattering angles by the Guinier law:[26]

$$\lim_{q\to 0} I_s(q) = I_s(0) \exp\left(-\frac{q^2 R_g^2}{3}\right) \qquad (4)$$

where $I_s(0)$ is the scattering at $q = 0$. R_g in eq 4 can be evaluated from a $\ln[I_s(q)]$ versus q^2 Guinier plot in the regime $qR_g < 1$.

Rheology. Rheological properties (flow experiments) were determined using a controlled stress TA Instruments AR-2000 rheometer (TA Instruments) equipped with a Mooney-Etward rotor (stator inner radius 13 mm, rotor outer radius 12.5 mm, gap 56 μm). Preliminary tests showed that this apparatus, operating in a shear mode, can accurately measure the shear viscosity of pure water within the range of shear stresses used in this study.

UV. The emission spectra of BSA, at an excitation wavelength of 280 nm, was recorded using a Perkin-Elmer LS50B luminescence spectrometer. Samples were mounted in 5 mm thick quartz cells. Emission spectra were obtained from 200 to 800 nm, using 60 s collection time.

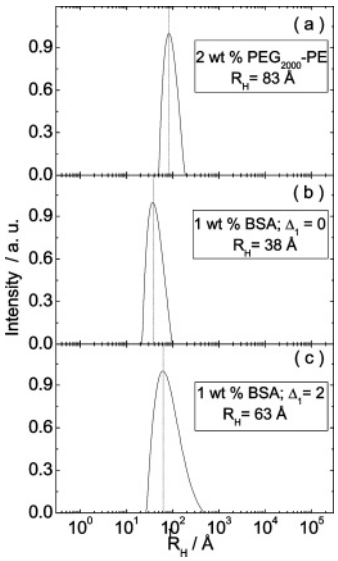

Figure 1. Hydrodynamic radii distributions, obtained at $\theta = 90°$, for samples containing (a) 2 wt % PEG_{2000}-PE, and 1 wt % BSA with (b) $\Delta_1 = 0$, (c) $\Delta_1 = 2$.

CD. Experiments were done using a Chirascan spectrometer (Applied Photophysics). Samples were mounted in a 0.1 mm thick quartz Hellma cells. The BSA concentration and the path length of the samples were chosen according to the absorbance value lower than 2 (a. u.) at any measured point.

Zeta-Potential. Eletrophoretic mobility was measured using a ZetaMaster (Malvern Instruments Ltd.). Measurements were performed five times for each sample. Zeta-potential, ζ, was determined from the electrophoretic mobility using the Smoluchowsky equation:[27]

$$\zeta = \frac{u_E \eta}{\epsilon_r e_o} \tag{5}$$

where u_E is the electro-osmotic mobility, ϵ_r is the dielectric constant, e_o is the permittivity of the vacuum, and η is the viscosity.

Results and Discussion

DLS experiments were performed on two different sets of samples. The first set of samples contained 1 wt % BSA with Δ_1 in the range (0−2), while the second set was free of protein and corresponded to polymer−lipid conjugate samples with 0.25−2 wt % PEG_{2000}-PE. As mentioned above, CONTIN program was used to calculate the decay rate and the particle radius distributions for $40 \leq \theta \leq 150°$. All the resulting distribution functions were characterized by only one peak. The position of the peak maximum in $G(\Gamma)$ and $A(R_H)$ curves was taken as the average decay rate $\bar{\Gamma}$ or hydrodynamic radius $\bar{R}_H$.

A representative example of particle radius distributions obtained at $\theta = 90°$ is shown in Figure 1 for a 2 wt % PEG_{2000}-PE sample and for samples containing 1 wt % BSA with $\Delta_1 = 0$ or 2.

It is possible to observe that the sample with 2 wt % PEG_{2000}-PE corresponds to micellar aggregates with $\bar{R}_H = 83$ Å (Figure 1a), in agreement with previous DLS results on 1.4 wt % PEG_{2000}-PE solutions with pH 7, obtained at room temperature.[20]

The sample containing 1 wt % BSA with $\Delta_1 = 0$ corresponds to $\bar{R}_H = 38$ Å (Figure 1b), in good agreement with the hydrodynamic micellar radius already reported in literature for monomeric BSA at pH 7.4.[28] Finally, the sample with 1 wt % BSA and $\Delta_1 = 2$ presents $\bar{R}_H = 63$ Å (Figure 1c), which is intermediate between the hydrodynamic radius of the BSA and the hydrodynamic radius of the PEG_{2000}-PE micelle. Results in Figure 1 suggest that in the presence of the protein, the PEG_{2000}-PE does not self-assemble to form a micelle but binds to the BSA, giving place to the formation of a protein/PEG-lipid complex.

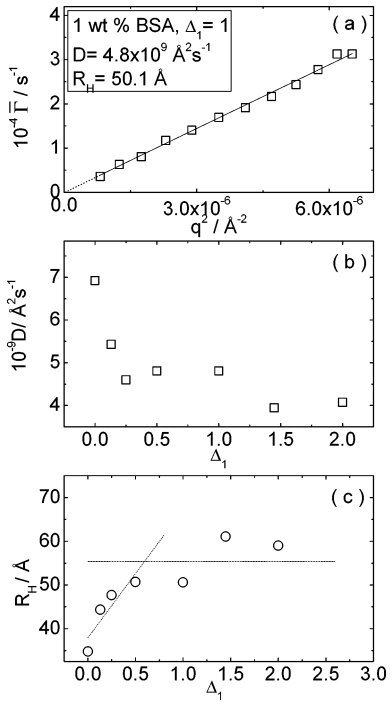

Figure 2. Variation of (a) decay rate $\bar{\Gamma}$ with q^2 (1 wt % BSA with $\Delta_1 = 1$). Dependence of (b) apparent diffusion coefficient D and (c) hydrodynamic radii R_H with Δ_1. The full line in part a is a fitting to the experimental data (see text), while the dotted line in part c is an extrapolation of the linear portions in the curve.

As mentioned above, CONTIN was used to calculate the relaxation rate distribution $G(\Gamma)$ as a function of the angle. All the resulting $G(\Gamma)$ functions were characterized by only one peak. The position of the peak maximum in $G(\Gamma)$ was taken as the average relaxation rate, $\bar{\Gamma}$, of the system. A representative result is shown in Figure 2a for a sample with 1 wt % BSA and $\Delta_1 = 1$. The dependence of $\bar{\Gamma}$ on q^2 could be fitted with a straight line with an intercept of zero, indicating a diffusive process time. The apparent diffusion coefficient D was calculated from the gradient of the $\bar{\Gamma}$ versus q^2 plot, and the hydrodynamic radius R_H was then obtained using eq 3.

The dependence of D and R_H with Δ_1, for the samples containing BSA, is shown in Figure 2b and Figure 2c, respectively. R_H calculated for samples with 0.25−2 wt % PEG_{2000}-PE was 86 Å with a corresponding diffusion time of 2.79×10^9 Å^2 s^{-1} (results not shown in Figure 2).

Results in Figure 2c show that although R_H steadily grows from 34.8 Å (for 1 wt % BSA with $\Delta_1 = 0$) to 59 Å (for 1 wt % BSA with $\Delta_1 = 2$), it always remains lower than R_H measured for PEG_{2000}-PE micelles ($R_H = 86$ Å). Results in Figure 2c are in good agreement with results in Figure 1, since they support the idea that PEG_{2000}-PE conjugates do not self-associate in the presence of protein; instead, the PEG-lipid is preferentially associated to the protein. In addition, results in Figure 2c show that the formation of complexes containing more than one BSA molecule is highly improbable in the BSA/PEG_{2000}-PE system.

A PEG_{2000} chain has a radius of gyration of 18 Å in aqueous solution at 20 °C, with a corresponding maximum length of 218 Å.[29] Simultaneously, the PE chain has a maximum length of 14 Å.[30] This provides a maximum length $l = (218 + 14)$ Å =

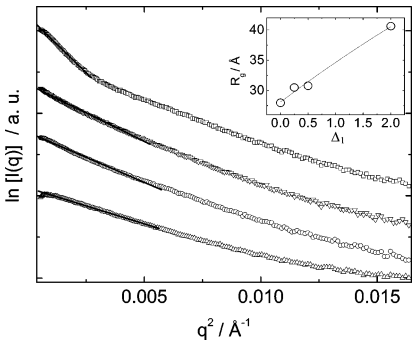

Figure 3. Guinier plots obtained for 1 wt % BSA with (△) $\Delta_1 = 0$, (○) $\Delta_1 = 0.25$, (▽) $\Delta_1 = 0.5$, or (□) $\Delta_1 = 2$. The SAXS curves have been shifted to enable the visualization of the data. The inset shows the dependence of the corresponding radii of gyration on Δ_1. The full line in the inset is a guide for the eyes.

232 Å for the PEG_{2000}-PE molecule. Thus, according to data in Figure 2c, the PEG_{2000}-PE conjugate adopts a folded configuration when it is associated to the BSA.

Data in Figure 2c shows that R_H increases with Δ_1 for low Δ_1 values, while R_H remains nearly independent of Δ_1 for high Δ_1 values. The extrapolation of the linear portions of the data in Figure 2c can be used to estimate the complex stoichiometry. The intersection of the two linear fittings in Figure 2c (corresponding to $\Delta_1 = 0.6$) can be taken as the onset of the complex stabilization. In this way, assuming that there is no free BSA or PEG-lipid in the BSA/$PEG2_{000}$-PE system, $\Delta_1 = 0.6$ provides a PEG_{2000}-PE bound to BSA molar ratio, $\beta = 14$.

It is possible to evaluate the accuracy in the estimation of β through the calculation of the refractive index increment for the binary BSA/PEG_{2000}-PE system. The value of β obtained from Figure 2c provides a theoretical refractive index increment[31] $(dn_o/dc)_T = 1/(1 + \beta^{-1})(dn_o/dc)_{PEG2000-PE} + [\beta^{-1}/(1 + \beta^{-1})]\ (dn_o/dc)_{BSA} = 0.138$ (using $(dn_o/dc)_{BSA} = 0.186$ mL/g and $(dn_o/dc)_{PEG2000-PE} = 0.134$ mL/g for the BSA[32] and the PEG_{2000}-PE[18], respectively). The experimental refractive index increment of the binary BSA/PEG_{2000}-PE system, $(dn_o/dc)_E = 0.13$, was measured using a thermostated Abbe refractometer. The parameter $(dn_o/dc)_E$ is only 6% different from $(dn_o/dc)_T$, showing a relatively high accuracy in the estimation of β.

SAXS experiments were undertaken on samples containing 1 wt % with $\Delta_1 = 0-2$. The SAXS intensity $I_s(q)$ was used to construct the Guinier plot for each sample (Figure 3). The SAXS curves in Figure 3 present only one Guinier region, showing that there is only one distribution of particle sizes in the system, in good agreement with DLS results. The radius of gyration of the scattering particle was calculated from the fitting of eq 4 to the SAXS data in Figure 3. The inset in Figure 3 shows the dependence of R_g on Δ_1. In agreement with data in Figure 2c, R_g increases with PEG_{2000}-PE concentration, from 28 Å ($\Delta_1 = 0$) to 40.6 Å ($\Delta_1 = 2$). The radius of gyration obtained here for the 1 wt % BSA sample at pH 7.4, free of PEG-lipid, is comparable to the published SAXS value of 30.6 Å[33] and small-angle neutron scattering value of 30.5 Å.[34]

A previous SAXS study in literature reported that, at neutral pH, the radius of gyration measured for BSA in water is higher than R_g measured using PEG as a cosolvent in the solution.[17] This results was ascribed to a PEG-depleted hydration layer around the protein.[17] In contrast, results in the inset of Figure 3 show an increment of R_g with increasing PEG_{2000}-PE concentration, suggesting that the presence of PE in the system avoids the formation of a depleted hydration layer around the BSA.

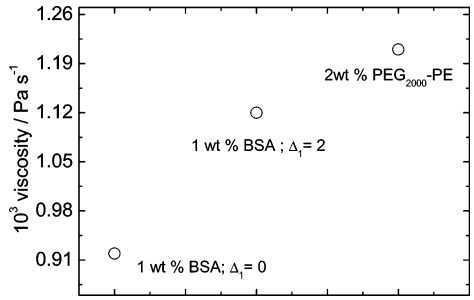

Figure 4. Shear viscosity measured for 1 wt % BSA ($\Delta_1 = 0$ and $\Delta_1 = 2$) and 2 wt % PEG_{2000}-PE solutions.

R_g increases with Δ_1 up to $\Delta_1 = 2$ (inset Figure 3), while R_H levels off at $\Delta_1 = 0.6$ (Figure 2c), suggesting that a structural change may occur at high Δ_1. However, it is not possible to draw any conclusion at this stage. Indeed, SAXS experiments covering a q range wider than that shown in Figure 3 have to be undertaken to provide detailed information about the shape of the scattering objects.

Rheology experiments were done on samples with 1 wt % BSA with $\Delta_1 = 0$ and $\Delta_1 = 2$ and on samples containing 2 wt % PEG_{2000}-PE. Flow experiments (Figure 4) showed that introduction of 1 wt % BSA in a 2 wt % PEG_{2000}-PE solution causes a reduction of the shear viscosity. This effect is consistent with the protein-induced disorganization of the micellar structure of PEG_{2000}-PE. If this was not the case, the viscosity of the hybrid system should increase rather than decrease. Moreover, additional rheological tests (not shown here) indicated a complex viscoelastic character of the PEG_{2000}-PE solutions (e.g., they exhibited a low but finite yield stress about 0.1 Pa when aged in the rheometer), while the protein-containing systems showed a typical Newtonian behavior. The viscosity of the complexes is intermediate between those of its components (Figure 4), suggesting that the complexes might be surrounded by a relatively compact PEG_{2000}-PE shell.

It is interesting at this stage to investigate the nature of the forces which drive the formation of BSA/PEG-lipid complexes. Our SAXS results have already shown that depletion forces do not seem to play an important role in the complex formation. A study reported in the literature about the formation of human serum albumin (HSA)/PEG agregates[35] shows that hydrogen bonding plays an important role in the complex formation. Consequently, it is possible to argue that BSA and PEG_{2000}-PE interact through the formation of H-bonds between the tryptophan (Trp) groups on the BSA surface and the PEG chains. This effect can be studied by fluorescence spectroscopy experiments. Therefore, UV experiments were done on samples containing 0.01 wt % BSA with $\Delta_2 = 0-50$. Following UV experiments in literature, made to study the HSA/PEG complexation,[35] the excitation wavelength in our work was fixed to $\lambda_{ex} = 280$ nm. Figure 5a shows the emission wavelength λ_{em} measured for $\Delta_2 = 0-50$.

The emission wavelength of Trp in aqueous solution is $\lambda_{em} = 350$ nm, while in a hydrophobic environment Trp emission occurs at $\lambda_{em} < 350$ nm. In particular, since BSA contains Trp groups, λ_{em} is usually shifted from shorter wavelengths to about 350 nm upon protein unfolding.

Figure 5a shows $\lambda_{em} = 348$ nm for $\Delta_2 = 0$, while there are two different regimes in λ_{em} for $\Delta_2 > 0$. For $0 < \Delta_2 < 1$, there is a blue shift of the $\lambda_{em} = 348$ nm measured for free BSA. The blue shift indicates that the Trp groups are exposed to an hydrophobic environment (probably consistent of the PE blocks), and it does not exclude the possible formation of H bonds between the Trp groups on the BSA surface and the PEG

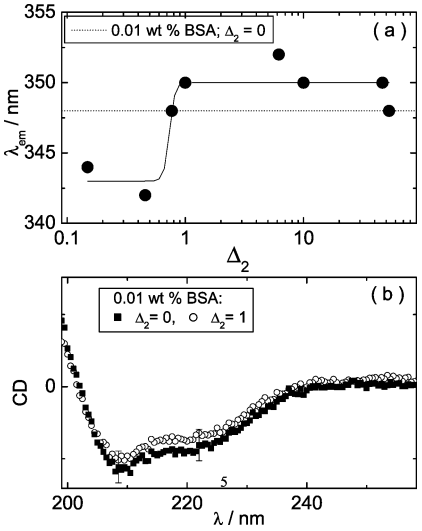

Figure 5. (a) UV emission wavelength measured as a function of Δ for aqueous BSA + PEG_{2000}-PE solutions. The dotted lines correspond to the emission wavelength measured for $\Delta_2 = 0$. The full line is a guide for the eyes. (b) CD spectra measured for samples with 0.01 wt % BSA and (■) $\Delta_2 = 0$ or (○) $\Delta_2 = 1$.

chains.[35] In contrast, Figure 5a shows that for $\Delta_2 > 1$ there is a red shift of the $\lambda_{em} = 348$ nm measured for free BSA. It is known that surfactants, such as sodium dodecyl sulfate, can unfold BSA.[36] Therefore, the red shift could be due to the unfolding of the BSA molecule, which subsequently means that the Trp groups are more likely to be exposed to the aqueous solution.

According to the paragraph above, it is expected that the secondary structure of the BSA can be affected because of the complexation with PEG_{2000}-PE. It is well-known that BSA is a protein with mainly α-helix secondary structure elements (59% in 10 mM phosphate buffer, pH 7.4).[37] Changes in its secondary structure can be easily detected by CD, which is sensitive to variations in the percentage of α-helix structure present in proteins structure. The CD spectrum for BSA in aqueous solution is characteristic of macromolecules with high α-helical content, monitored by the two well-defined ellipticities values at 208 and 222 nm.[38] In our work, the CD spectrum was measured for the same set of concentrations studied using UV experiments.

Figure 5b shows some representative results, corresponding to the CD spectra obtained for samples with 0.01 wt % BSA and $\Delta_2 = 0$ or 1. Results in Figure 5b present the two distinctive negative bands for BSA, situated at 208 and 222 nm. However, variations in CD spectra with Δ_2 purely arise because of inherent experimental error (Figure 5b), without denoting any particular trend in the dependence of the secondary structure of BSA on Δ_2.

According to our data, the initial binding of PEG_{2000}-PE to BSA at low PEG-lipid concentrations results in a blue shift of the UV-spectra. At higher PEG_{2000}-PE concentrations, the Trp groups are exposed to the water leading to a red shift of the UV-spectra. However, it was not possible to measure any important change in the secondary structure of the BSA induced by variations of the PEG-lipid concentrations, as denoted by CD curves in Figure 5b.

It is known that BSA can unfold losing only ~9% of its α-helix secondary structure elements.[39] Therefore, although the red shift measured by UV ($\Delta_2 > 1$) can be associated to BSA unfolding, the protein might still have a relative high α-helix secondary structure content for $\Delta_2 > 1$ (Figure 5a). Consequently, a minor change in the secondary structure of BSA upon increasing $c_{PEG2000-PE}$, for $\Delta_2 > 1$, is screened by the high α-helix secondary structure content and cannot be measured by CD.

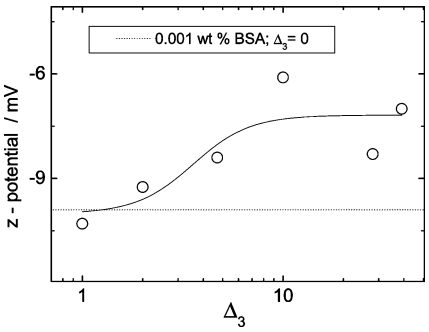

Figure 6. Dependence of the zeta-potential on Δ_3. The dotted lines correspond to the zeta-potential measured for $\Delta_3 = 0$. The full line is a guide for the eyes.

CD and UV studies on the formation of BSA/sodium dodecyl sulfate (SDS) complexes at pH 7 have been reported in the literature.[36] Similarly to the UV results discussed above, it was found that Trp groups are exposed to SDS for low surfactant concentrations, while higher SDS concentrations expose Trp groups to water, leading to BSA unfolding. However, according to CD results in ref 36, the percentage of protein denaturation induced by SDS is much higher than that reported in our work.

Figure 6 shows the results obtained for the zeta-potential measured for samples with 0.001 wt % BSA and $\Delta_3 = 0-39$. The protein concentration was chosen according to data provided in the literature for similar experiments performed at pH 7.4[40,41] to ensure that concentration effects would not affect the final result. The zeta-potential measure for 0.001 wt % BSA was −9.9 mV. Previous studies reported a zeta-potential value of −35 mV for $I = 0.1$ M, pH 7.4, and 0.0001 wt % BSA.[40,41] For our sample, higher zeta-potential values correspond to higher ionic strengths ($I = 0.169$ M).

Figure 6 shows that the zeta-potential becomes gradually less negative upon increasing Δ_3. Probably, polymer−lipid conjugate adsorption on the protein surface reduces the electrostatic interaction while enhancing the steric stabilization and contributes toward the stabilization of the BSA/PEG_{2000}-PE complexes.

Conclusions

In this work, we have described the complexation of BSA with PEG_{2000}-PE, within three different concentration intervals with fixed c_{BSA} and variable $c_{PEG2000-PE}$, namely, Δ_1 (c_{BSA} = 1 wt %), Δ_2 (c_{BSA} = 0.01 wt %), and Δ_3 (c_{BSA} = 0.001 wt %).

In the Δ_1 interval, DLS has shown that when BSA is added to PEG_{2000}-PE micellar solutions, the structure of the micelles is disrupted, and BSA/PEG_{2000}-PE aggregates, with a size intermediate between the BSA monomer and the polymer conjugate micelles, are present in the solution. The size of BSA/PEG_{2000}-PE complexes increases upon increasing Δ_1, until the complexes reach a stable size for $\Delta_1 \sim 0.6$. Flow viscosity experiments denoted the formation of BSA/PEG_{2000}-PE complexes upon mixing the corresponding compounds in solution such that the complexes might be surrounded by a relatively compact PEG-lipid shell. SAXS could be used to rule out the possibility of depletion forces taking part in the stabilization of the BSA/PEG_{2000}-PE complex.

UV experiments in the Δ_2 range proved the existence of two different regimes for the Trp groups in the BSA. At low PEG-

lipid concentrations, the Trp groups are exposed to a hydrophobic environment probably represented by the PE group of the PEG_{2000}-PE. At high PEG-lipid concentrations, the Trp groups are exposed to water. CD results show that this change of environment for the Trp groups in the Δ_2 range takes place with a minimal alteration of the BSA secondary structure elements.

Zeta-potential results in the Δ_3 regime have shown that steric interactions might play an important role in the stabilization of the BSA/PEG_{2000}-PE complex. In addition, it is highly probable that the complexes are stabilized by hydrophobic forces, driven by the high hydrophobicity of the PE block in the polymer−lipid conjugate.

Acknowledgment. V.C. would like to acknowledge Ms. Maria Dermiki for her support during the zeta-potential experiments, Professor J. Gibbins for providing the facilities for the UV experiments, Professor I. W. Hamley for giving access to the CD and DLS machines, and Dr. I. Abbas for helpful discussions. V.C. was supported by a U.K. Relocation Fellowship from the Royal Society.

References and Notes

(1) Kokufuta, E. *Macromolecular Complexes in Chemistry and Biology*; Springer-Verlag: Heidelberg, Germany, 1993.
(2) Bozzano, A. G.; Andrea, G.; Glatz, C. E. *J. Membr. Sci.* **1991**, *55*, 181.
(3) Dubin, P. L.; Gao, J.; Mattison, K. *Sep. Purif. Methods* **1994**, *23*, 1.
(4) Margolin, A.; Sheratyuk, S. F.; Izumrudov, V. A.; Zezin, A. B.; Kabanov, V. A. *Eur. J. Biochem.* **1985**, *146*, 625.
(5) Ruckpoul, K.; Rein, H.; Janig, G. R.; Pfeil, W.; Ristau, O.; Damaschun, B.; Damaschun, H.; Muller, J. J.; Purschel, H. V.; Bleke, J.; Scheler, W. *Stud. Biophys.* **1972**, *34*, 81.
(6) Hughes, W. L. *The Proteins*; Academic Press: New York., 1954; Vol. 2.
(7) Squire, P. G.; Moser, P.; O'Konski, C. T. *Biochemistry* **1968**, *7*, 4261.
(8) Wright, A. K.; Thompson, M. R. *Biophys. J.* **1975**, *15*, 137.
(9) Bloomfield, V. *Biochemistry* **1966**, *5*, 684.
(10) Bos, O. J. M.; Labro, J. F. A.; Fischer, M. J. E.; Witling, J.; Janssen, L. H. M. *J. Biol. Chem.* **1989**, *264*, 953.
(11) Carter, D. C.; He, X. M.; Munson, S. H.; Twigg, P. D.; Gernert, K. M.; Broom, M. B.; Miller, T. Y. *Science* **1989**, *244*, 1195.
(12) Riley, D. P.; Oster, G. *Discuss. Faraday Soc.* **1951**, *11*, 107.
(13) Doherty, P.; Benedek, G. B. *J. Chem. Phys.* **1974**, *61*, 5426.
(14) Bendedouch, D.; Chen, S.-H. *J. Phys. Chem.* **1983**, *87*, 1473.
(15) Matsudo, T.; Ogawa, K.; Kokufuta, E. *Biomacromolecules* **2003**, *4*, 1794.
(16) Peters, R.; Sikorski, R. *Science* **1999**, *286*, 434.
(17) Murthy, N. S.; Knox, J. R. *Biopolymers* **2004**, *74*, 457.
(18) Johnsson, M.; Hansson, P.; Edwards, K. *J. Phys. Chem. B* **2001**, *105*, 8420.
(19) Gao, Z.; Lukyanov, A. N.; Singhal, A.; Torchilin, V. P. *Nano Lett.* **2002**, *9*, 979.
(20) Lukyanov, A. N.; Gao, Z.; Torchilin, V. P. *J. Controlled Release* **2003**, *91*, 97.
(21) Peters, T., Jr. *Adv. Protein Chem.* **1985**, *37*, 161.
(22) Barbosa, S.; Leis, D.; Taboada, P.; Attwood, D.; Mosquera, V. *Mol. Phys.* **2002**, *100*, 3367.
(23) Kragh-Hansen, U. *Pharmacol. Rev.* **1981**, *33*, 17.
(24) Berne, B. J.; Pecora, R. *Dynamic Light Scattering*; Wiley-Interscience: New York, 1976.
(25) Provencher, S. W. *Makromol. Chem.* **1979**, *180*, 201.
(26) Glatter, O.; Kratky, O. *Small Angle X-ray Scattering*; Academic: London, 1982.
(27) Fennel Evans, D.; Wennerstrm, H. *The colloidal domain. Where physics, chemistry and biology meet;* New York, 1994.
(28) Martinez-Landeira, P.; Ruso, J. M.; Prieto, G.; Sarmiento, F.; Jones, M. N. *Langmuir* **2002**, *18*, 3300.
(29) Bhat, R.; Timasheff, S. N. *Protein Sci.* **1992**, *1*, 1133.
(30) Tanford, C. *J. Phys. Chem.* **1972**, *76*, 3020.
(31) Xia, J.; Dubin, P. L.; Dautzenberg, H. *Langmuir* **1993**, *9*, 2015.
(32) Doty, P. *Adv. Protein Chem.* **1951**, *6*, 35.
(33) Luzzati, V.; Witz, J.; Nicolaieff, A. J. *J. Mol. Biol.* **1961**, *3*, 379.
(34) Bendedouch, D.; Chen, S.-H. *J. Phys. Chem.* **1983**, *87*, 1473.
(35) Azegami, S.; Tsuboi, A.; Izumi, T.; Hirata, M.; Dubin, P. L.; Wang, B.; Kokufuta, E. *Langmuir* **1999**, *15*, 940.
(36) Deep, S.; Ahluwalia, J. C. *Phys. Chem. Chem. Phys.* **2001**, *3*, 4583.
(37) Norde, W.; Giacomelli, C. E. *J. Biotechnol.* **2000**, *79*, 259.
(38) Kelly, S. M.; Price, N. C. *Biochim. Biophys. Acta* **1997**, *161*, 1338.
(39) Lee, C. T.; Smith, K. A.; Hatton, T. A. *Biochemistry* **2005**, *44*, 524.
(40) Fuda, E.; Jauregi, P. *J. Chromatogr., B* **2006**, *843*, 317.
(41) Fuda, E.; Jauregi, P.; Pyle, D. L. *Biotechnol. Prog.* **2004**, *20*, 514.

BM070116O